INTERNATIONAL JOURNAL OF IMMINENT SCIENCE & TECHNOLOGY
Journal homepage: www.ijisnt.com
ISSN.3006-3116
2023 Vol-2 Issue-1

Efficiency Enhancement of Lead-Free $CsSnGeI_3$-Based Perovskite Solar Cells Using ZnSe as an Electron Transport Material and Spiro-MeOTAD as the Hole Transport Material

[1]Monira Khanom Mim, [2]Sunirmal Kumar Biswas, [3]Maruf Rahman Shuvo, [4]Md. Nazmul Islam
[1]moniramim2@gmail.com, [2]sujan.ru.apee@gmail.com, [3]marufrahmanshuvo@gmail.com, [4]nazmulislam1581@gmail.com

[1,2,3,4]Department of Electrical and Electronic Engineering, Prime University

Abstract

Perovskite solar cells are an emerging technology in the field of photovoltaic cells, they have higher efficiency, relatively low production cost, and are more versatile than traditional silicon solar cells. In this research, a cesium tin–germanium triiodide ($CsSnGeI_3$) perovskite solar cell has achieved high power conversion efficiency and extreme air stability. In this study, lead-free Cs-based perovskite solar cells have been quantitatively analyzed to explore the effect of absorber layer thickness, defect density of the absorber layer, working temperature, series and shunt resistance, acceptor doping concentration using a solar cell capacitance simulator software. For this perovskite solar cell structure, ZnSe is used as a buffer layer, and CsSnGeI3 is used as an absorber layer. ITO material is used as an electron transport layer and Spiro-MeOTAD Transport Layer. Gold is used to make the back contact of this proposed solar cell. In this simulation, the environment-friendly perovskite solar cell achieved an efficiency of 31.22% when the thickness of the buffer and absorber layers was 0.06µm and 1.5µm. The designed outputs will be efficient for the convenient fabrication of the perovskite solar cell.

Keywords -Renewable Energy, Solar Energy, Perovskite solar cell, Eco-friendly

1. Introduction

Today, the world still heavily relies on fossil fuels and even continues subsidizing them. Renewable energy is derived from natural resources that replenish themselves in less than a human lifetime without depleting the planet's resources. Transitioning from fossil fuels to renewable energy is fundamental for halting anthropogenic climate change [1]. The world's energy demand is growing fast because of the population explosion and technological advancements. It is therefore important to go for reliable, cost-effective, and everlasting renewable energy sources for future energy demand. Solar energy, among other renewable sources of energy, is a promising and freely available energy source for managing long-term issues in energy crises. The solar industry is developing steadily all over the world because of the high demand for energy. In contrast, the major energy source, fossil fuel, is limited, and other sources are expensive [2]. Hybrid organic-inorganic perovskite solar cells (PSCs) have recently emerged as a promising photovoltaic (PV) candidate [3,4] . Apart from the solar cell, perovskite materials have many applications in other optoelectronic devices, such as light-emitting diodes [5,6,7], photodetector [8], and photodiode [9]. However, lead toxicity [10,11], which has various health and environmental hazards, is the major hurdle in commercial applications of perovskite solar cells [12]. Alloys of Ge and Sn represent promising materials, with an advantageous gap for optoelectronic applications and higher stability than pure Sn-based perovskite [13]. Elements like Sn, Bi, and Ge take over Perovskite solar cells in PSCs [14]. Among these tin-based ($CsSnI_3$) candidates, Perovskite becomes the most promising [14,15]. However, the self-oxidation of Sn from Sn^{2+} to Sn^{4+} and phase instability in the $CsSnI_3$ perovskite prevent further application as a solar cell [16]. Recently, Min Chen et al. have reported that alloying CsSnI3 with Ge (II) to form a

DOI: https://doi.org/10.70774/ijist.v2i2.23

INTERNATIONAL JOURNAL OF IMMINENT SCIENCE & TECHNOLOGY
Journal homepage: www.ijisnt.com
ISSN.3006-3116

$CsSn_{0.5}Ge_{0.5}I_3$ gives a highly stable and air-tolerant perovskite solar cell [17].

Proper choice of HTMs (Hole Transport Material) is a key factor for efficient charge extraction and stability and contributes to charge transportation from Perovskite to back contact [18,19]. Spiro-MeOTAD is proven to be the most suitable for HTL material [20]. HTM for testing PSCs due to its facile implementation and high performance. Similarly, Spiro-MeOTAD is receiving attention in other applications other than solar cells due to its desirable properties [21]. ZnSe is an important technical optoelectronic semiconductor with a large 2.7 eV bandgap. ZnSe can be substituted in solar photovoltaic cells. Due to its potential applications in several optical and electronic devices and as a buffer/window material for thin film-heterojunction solar cells, it is seen as an important technological material [22].

In this simulation, we introduced a perovskite solar cell that has $CsSnGeI_3$ as the absorber layer and ZnSe as a buffer layer. For the ETL and HTL layer, ITO and Spiro-MeOTAD are used. After performing the simulation, a high efficiency of 31.2% was gained. This solar cell can be recommended for its high efficiency and nontoxic elements.

2. Numerical simulation and parameters of materials

The numerical modelling of the devices enables us to understand the solar cell dynamics without the need for actual manufacturing. It also provides a high-level outline of the device's functionality [23]. The one-dimensional SCAPS was used in this simulation study. The continuity equation and Poisson's equation are given for the free electrons and holes in the conduction and valence bands [24]. Hole and electron continuity equations are

$$-\frac{1}{q}\frac{d_{jn}}{dx} - U_n + G = \frac{d_n}{dt} \quad (1)$$

$$-\frac{1}{q}\frac{d_{jp}}{dx} - U_p + G = \frac{d_p}{dt} \quad (2)$$

Where Jn and Jp are electron and hole current densities and G is the generation rate. The Poisson equation is

$$\frac{d^2}{dx^2}\psi(x) = \frac{\theta}{\epsilon_0\epsilon_r}(\rho(x) - n(x) + N_D - N_A + \rho_p - \rho_n) \quad (3)$$

Where ψ is the electrostatic potential, e is the electrical charge, ε_r is the relative, and ε_0 is the vacuum permittivity, p and n are the concentrations of holes and electrons, respectively, N_A and N_D are the charge impurities of the acceptor and donor types, and ρ_p and ρ_n are the distributions of holes and electrons. SCAPS is a very powerful software for performing solar cells, and a description of the program and the algorithms it uses is found in the literature and its user manual [25,26,27]. Figure 1 shows the schematic diagram of the proposed perovskite solar cell structure. According to the references, the ITO, ZnSe, $CsSnGeI_3$ and Spiro-MeOTAD thin film parameters used to run our numerical simulations are listed in Table 1.

DOI: https://doi.org/10.70774/ijist.v2i2.23

INTERNATIONAL JOURNAL OF IMMINENT SCIENCE & TECHNOLOGY
Journal homepage: www.ijisnt.com
ISSN:3006-3116
2023 Vol-2 Issue-1

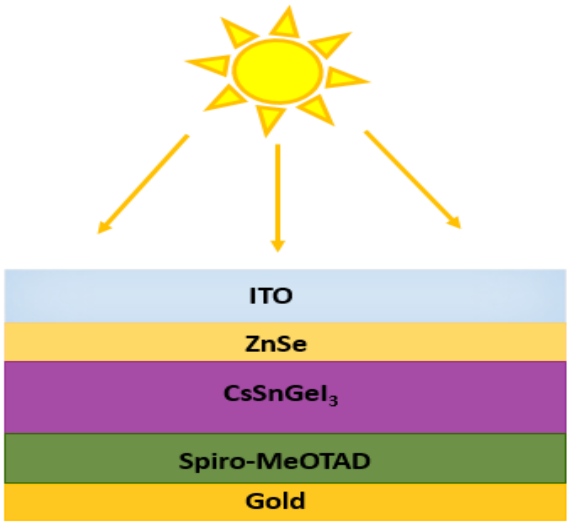

Figure 1. Schematic diagram of the proposed perovskite solar cell.

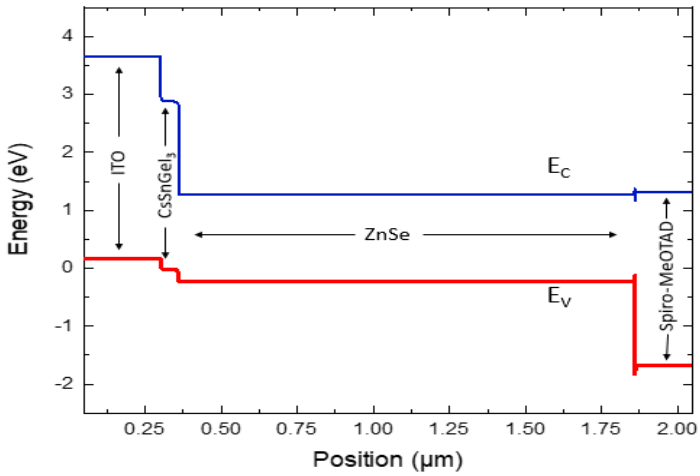

Figure 2. (a) Energy band diagram of the proposed solar cell

The energy band diagram for the suggested perovskite solar cell was extracted using the SCAPS-1D software.

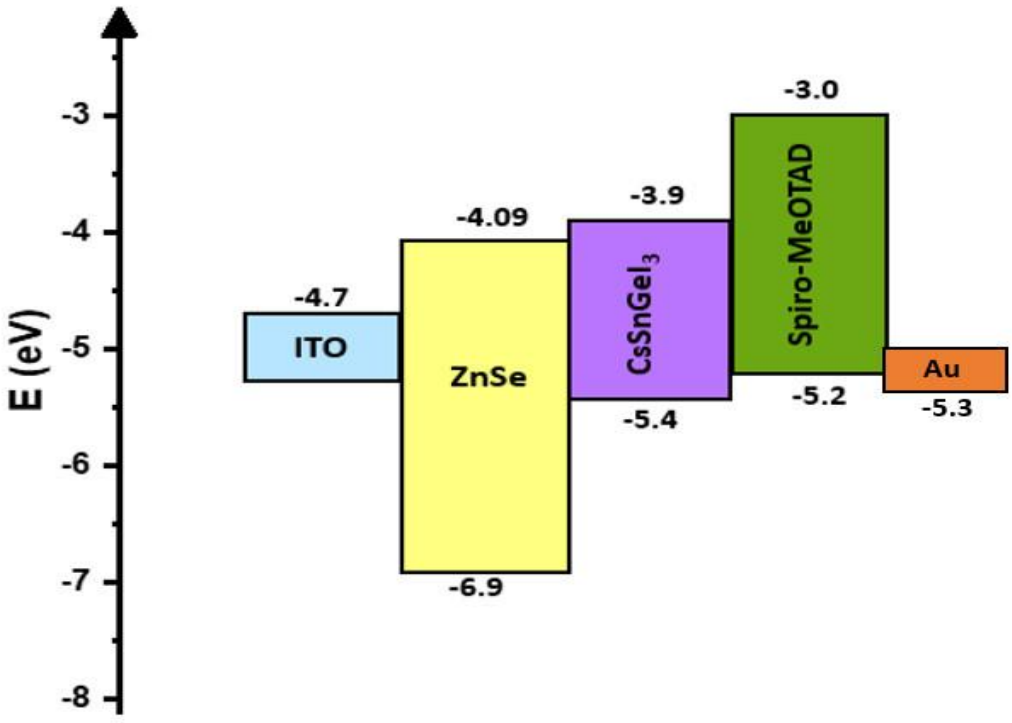

Figure-2 (b) Energy band alignment for different material used in Perovskite solar cell

DOI: https://doi.org/10.70774/ijist.v2i2.23

INTERNATIONAL JOURNAL OF IMMINENT SCIENCE & TECHNOLOGY
Journal homepage: www.ijisnt.com
ISSN.3006-3116

The energy band diagram, depicted in Figure 2(a), discusses solar cells optical properties. Figure-2 (b) shows the energy band alignment for different material used in Perovskite solar cell

Material Parameter	ITO	ZnSe	$CsSnGeI_3$	SpiroMeOTAD
Thickness (µm)	0.3	0.06	1.5	0.2
E_g (eV)	3.5	2.9	1.5	3
E_a(eV)	4	4.02	3.9	2.2
ε (relative)	9	10	28	3
CB(cm^{-3})	$2.2x10^{18}$	$2.2x10^{18}$	$3.1x10^{18}$	$2.2x10^{18}$
VB(cm^{-3})	$1.8x10^{19}$	$1.8x10^{19}$	$3.1x10^{19}$	$1.8x10^{19}$
μ_m (cm^2/V-s)	20	25	$9.74x10^{2}$	$2.1x10^{-3}$
μ_p(cm^2/V-s)	100	100	$2.13x10^{2}$	$2.16x10^{-3}$
N_D (cm^{-3})	$1x10^{21}$	$1x10^{18}$	0	0
N_A (cm^{-3})	0	0	$1x10^{19}$	$1x10^{18}$

Table 1: Parameters used in SCAPS-1D simulation

3. Result and Discussion

3.1. Impact of Absorber layer thickness

The impact of the absorber layer's thickness and band gap is shown in Figure 3(a) for solar cell performance metrics such as efficiency, fill factor, open circuit voltage, and short circuit current. One of the essential factors in improving solar cells' efficiency is the absorber layer's thickness [28,29]. All parameters of the solar cell are increased with the absorber layer or $CsSnGeI_3$ thickness. Here, thickness is varied from 0.5 µm to 3 µm. Figure 3(a) shows the effect of absorber layer variation on solar cell parameters. Efficiency increases from 28.46% to 31.35%. This might be caused by the fact that as the absorber layer becomes thicker, more short-wavelength photons are absorbed, which increases the photo generation of more free carriers [30]. J_{sc} increases from 25.42 to 28.64 mA/cm^2. J_{sc} increases with the increasing thickness, which is attributed to the generation of more electron-hole pairs in the perovskite, leading to an efficiency enhancement. But V_{oc} decreased from 1.25 to 1.22V, which is almost negligible. The decrease in V_{oc} with the thickness is attributed to the increment in the dark saturation current, which increases the recombination of the charge carriers [31]. That can be explained by the dependency of open-circuit voltage on the photo-generated current and dark saturation current, which is written as [32]

$$V_{OC} = \frac{kT}{q}\ln(1 + \frac{J_{sc}}{J_0}) \quad (4)$$

Where kT/q is the thermal voltage, J_{sc} is the photo-generated current density, and J_0 is the saturation current density.

DOI: https://doi.org/10.70774/ijist.v2i2.23

INTERNATIONAL JOURNAL OF IMMINENT SCIENCE & TECHNOLOGY
Journal homepage: www.ijisnt.com
ISSN.3006-3116
IJIST 2023 Vol-2 Issue-1

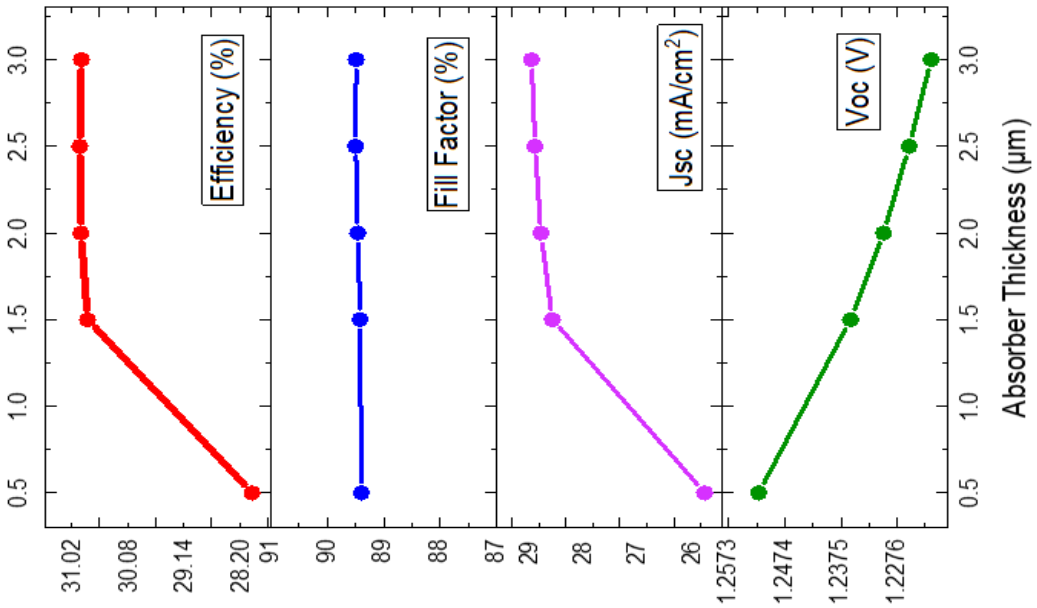

Figure 3(a): Effect of absorber layer thickness on solar performance parameter.

Quantum efficiency is the ratio of carriers captured **by** the solar cell to photons incident on the solar cell at a given energy [33]. The quantum efficiency curve of the proposed perovskite solar cell is shown in Figure 3(b) on the thickness of the absorber layer ranges from 0.5µm to 3µm. Figure 3(c) shows that the current density-voltage curve decreases with the increase of absorber layer thickness.

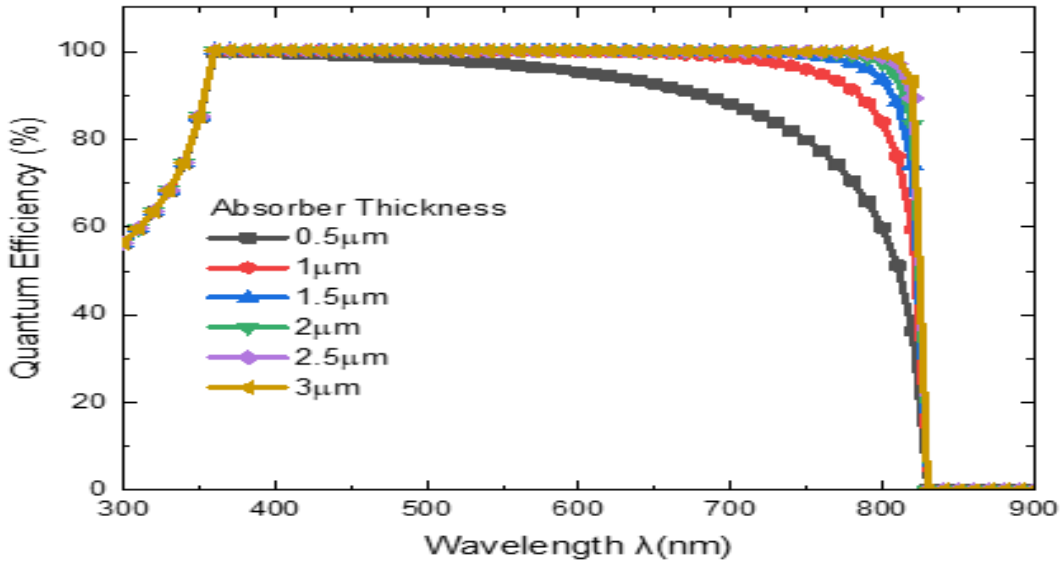

Figure 3(b): Effect of absorber layer thickness on quantum efficiency.

Figure 3(b) shows that the Quantum Efficiency rises at longer wavelengths when the absorber layer thickness

DOI: https://doi.org/10.70774/ijist.v2i2.23

INTERNATIONAL JOURNAL OF IMMINENT SCIENCE & TECHNOLOGY
Journal homepage: www.ijisnt.com
ISSN.3006-3116
IJIST 2023 Vol-2 Issue-1

increases. This is because, inside the absorber layer, photons cannot generate sufficient electron-hole pairs [34].

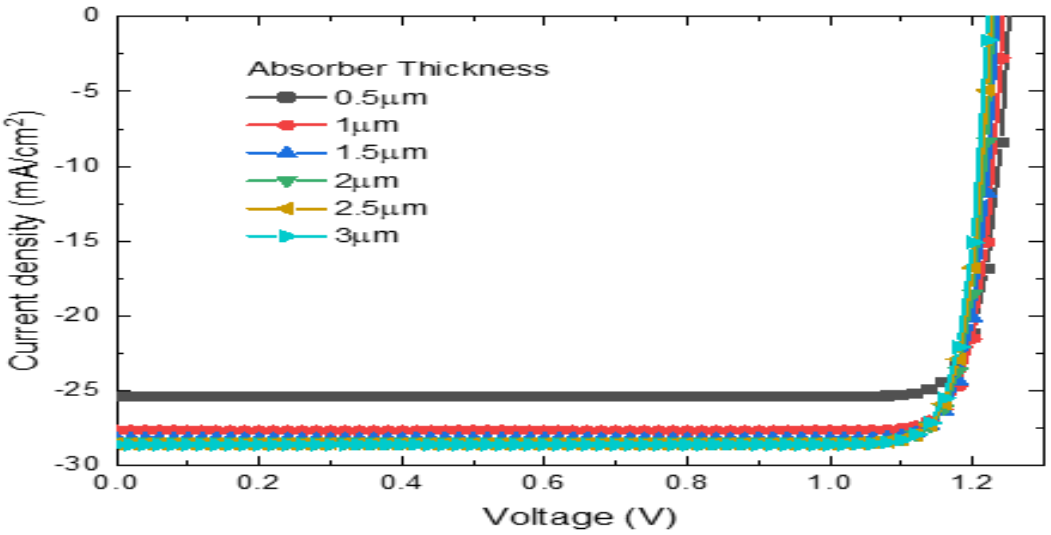

Figure 3(c): Effect of absorber layer thickness on current density-voltage.

3.2. Effect of defect density of the absorber layer

The defects in the solar cell's material play a very important role. The defects create an intermediate energy level between the conduction band and valance band and work as a recombination center [35, 36]. Figure 4 shows the effect of absorber layer defect density on the parameters of solar cells. The defect is varied from $2.4x10^{13}$ to $2.4x10^{17}$ cm^{-3}. V_{oc} decreases from 1.27 to 1.07V, J_{sc} 28.26 to 21.33 (mA/cm^2), FF 89.19% to 86.77%, and efficiency from 32.03% to 22.78%. Thus, increasing the defects in the material will increase the recombination [37]. The defect reduces the diffusion length and lifetime of the charge carrier, thus reducing the collection probability of the generated carrier by the junction [38].

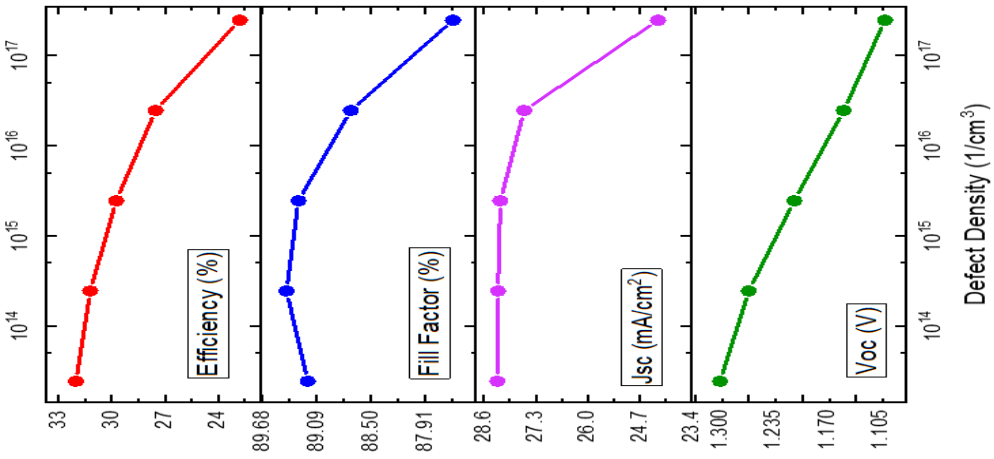

Fig 4(a): Effect of defect density of absorber layer on solar performance parameter.

Figure 4(b) demonstrates the influence of defect density in the absorber layer on the quantum efficiency of perovskite solar cells, which has been investigated by changing defect density from $2.45x10^{13}$ to $2.45x10^{17}$.

DOI: https://doi.org/10.70774/ijist.v2i2.23

INTERNATIONAL JOURNAL OF IMMINENT SCIENCE & TECHNOLOGY
Journal homepage: www.ijisnt.com
ISSN.3006-3116

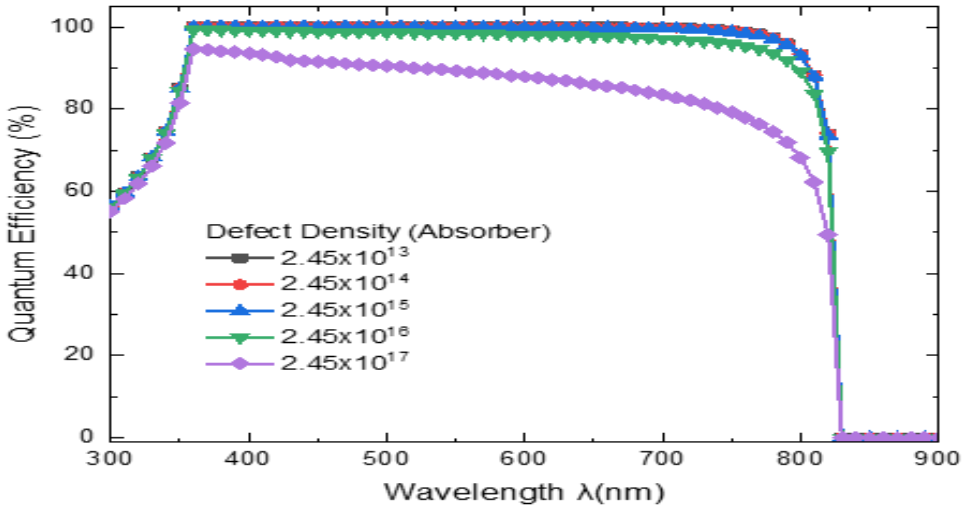

Fig 4(b): Effect of defect density of absorber layer on quantum efficiency.

From Figure 4(b), it can be observed that when the defect density is $2.45x10^{13}$, the quantum efficiency is about 100% in the range of wavelengths from 380 to 830 nm. When the defect density $2.45x10^{17}$ quantum efficiency is about 95% lower, the defect density affects the recombination of the photo-generated electron-hole pairs in the absorber layer. After the simulation, the optimum defect was gained at $2.45x10^{14}$.

Figure 4(c) shows the effect of defect density in the absorber layer on the current density-voltage of the proposed perovskite solar cell. From Figure 4 (c), the device performance relied heavily on the absorber defect density. With increasing defect density, the recombination rate also increases, reducing the power conversion efficiency. The higher defect densities of the two interfaces bring more traps and recombination centers and deteriorate the performance of cells. [39].

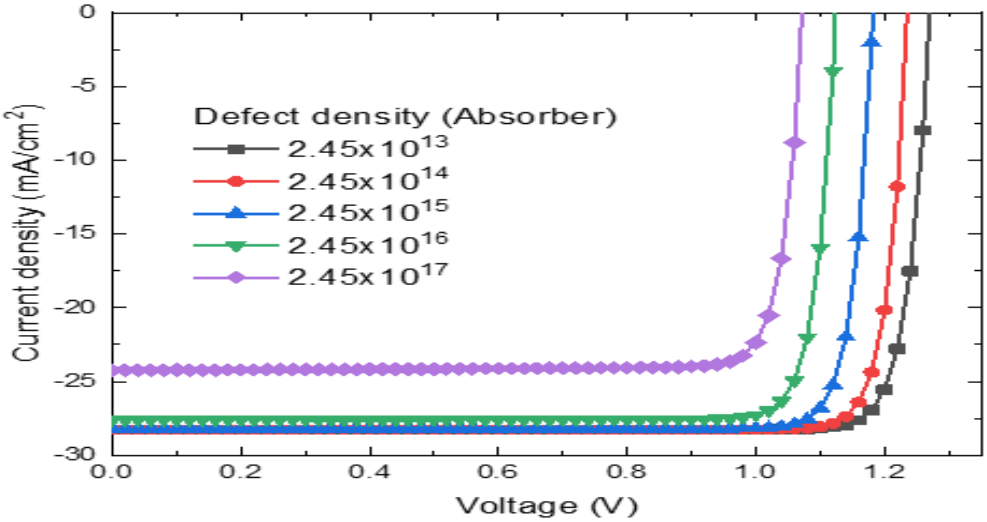

Fig 4(c): Effect of defect density of absorber layer on current density-voltage.

3.3. Effect of the operating temperature

The operating temperature always plays a vital role in the performance of a device. It has been reported that temperature augmentation increases strain and stress in

DOI: https://doi.org/10.70774/ijist.v2i2.23

INTERNATIONAL JOURNAL OF IMMINENT SCIENCE & TECHNOLOGY
Journal homepage: www.ijisnt.com
ISSN.3006-3116
IJIST 2023 Vol-2 Issue-1

structures. It results in increased interfacial defects, disorder, and poor interconnectivity between layers.

Figure 5(a) shows the effect of temperature on the proposed perovskite solar cell. The simulation operating temperature was varied from 250K to 450K by keeping all other parameters constant. In Figure 5(a), as temperature increases, efficiency drops from 32.71% to 25.19%. Similarly, FF was 89.88% to 84.34%, and V_{oc} was 1.28 to 1.05V. But it is observed that J_{sc} slightly increases. This is due to the energy band gap reduction and to more electron-hole pairs generation. In addition, when the device is running at a higher temperature, the bandgap gets smaller, which may lead to more excitation recombination and less efficiency [40]

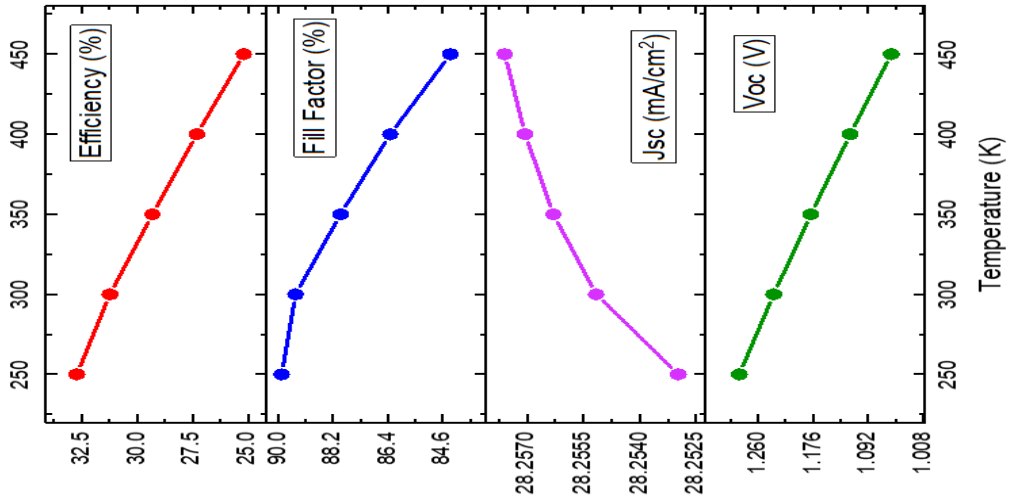

Figure 5(a): Effect of temperature on solar performance parameter

It's also observed that in Figure 5(b), the quantum efficiency doesn't change significantly. Figure 5(c) shows that the current density-voltage on the temperature of the proposed perovskite solar cell [41].

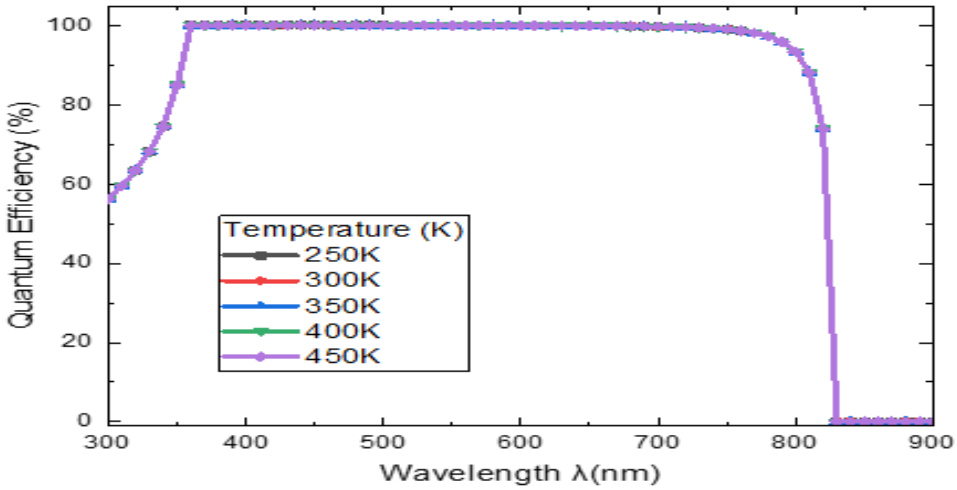

Figure 5(b): Effect of temperature on quantum efficiency.

DOI: https://doi.org/10.70774/ijist.v2i2.23

INTERNATIONAL JOURNAL OF IMMINENT SCIENCE & TECHNOLOGY
Journal homepage: www.ijisnt.com
ISSN:3006-3116

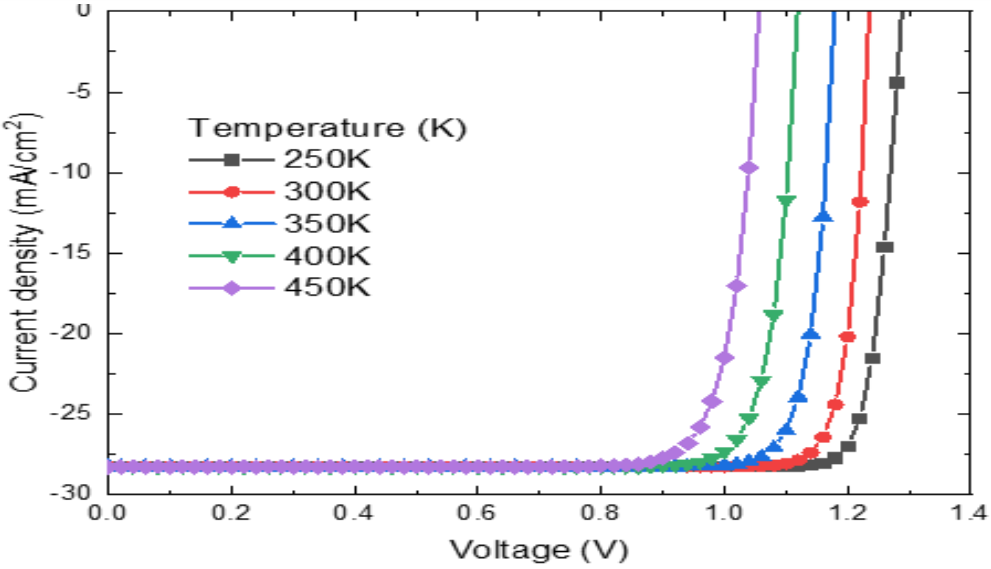

Figure 5(c): Effect of temperature on current density-voltage.

3.4. Effect of series resistance

The series resistance (Rs) significantly affects the operation of the proposed solar cell [42]. Figure 6(a) shows the effect of series resistance on the performance parameter of solar cell.

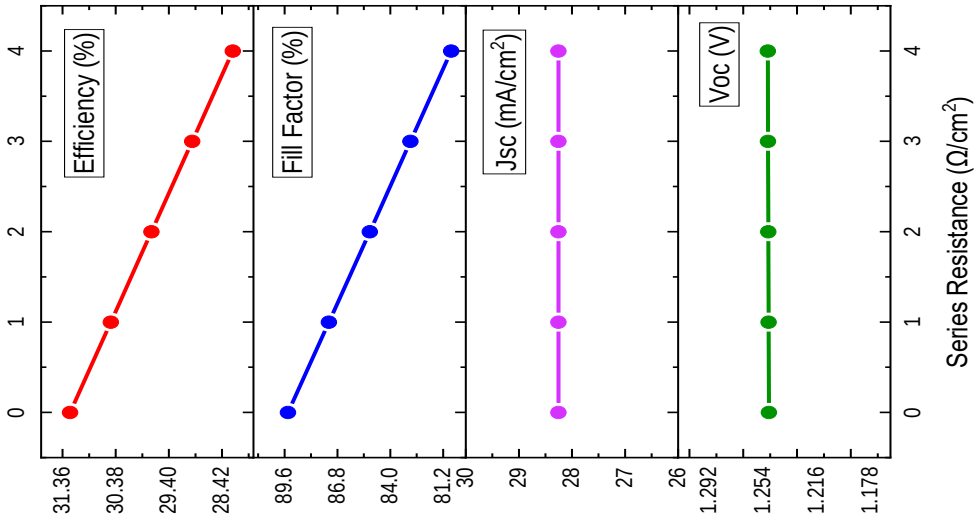

Figure 6 (a) Effect of series resistance on proposed solar cell on solar performance parameter

In this simulation series, resistance is varied from 0 to 4 Ω. Shunt resistance was fixed at $1x10^7$ Ω. Figure 6(a) shows the effect of resistance on Voc, Jsc, FF, and efficiency. Efficiency decreased from 31.22% to 28.22%. The efficiency of the devices deteriorates rapidly as the Rs rises. These findings are consistent with those reported in other studies [43,44].

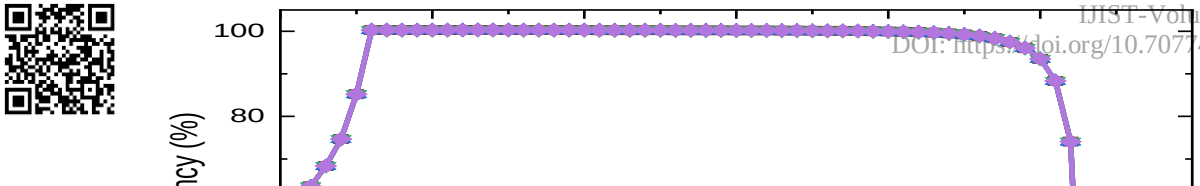

IJIST-Volume-2, Issue-1
DOI: https://doi.org/10.70774/ijist.v2i2.23

INTERNATIONAL JOURNAL OF IMMINENT SCIENCE & TECHNOLOGY
Journal homepage: www.ijisnt.com
ISSN.3006-3116

Figure 6 (b) Effect of series resistance on proposed solar cell on quantum efficiency.

The quantum efficiency doesn't vary with the variation of series resistance, as shown in Figure 6(b). Current density- voltage curve is decreased, as shown in Figure 6(c) [45].

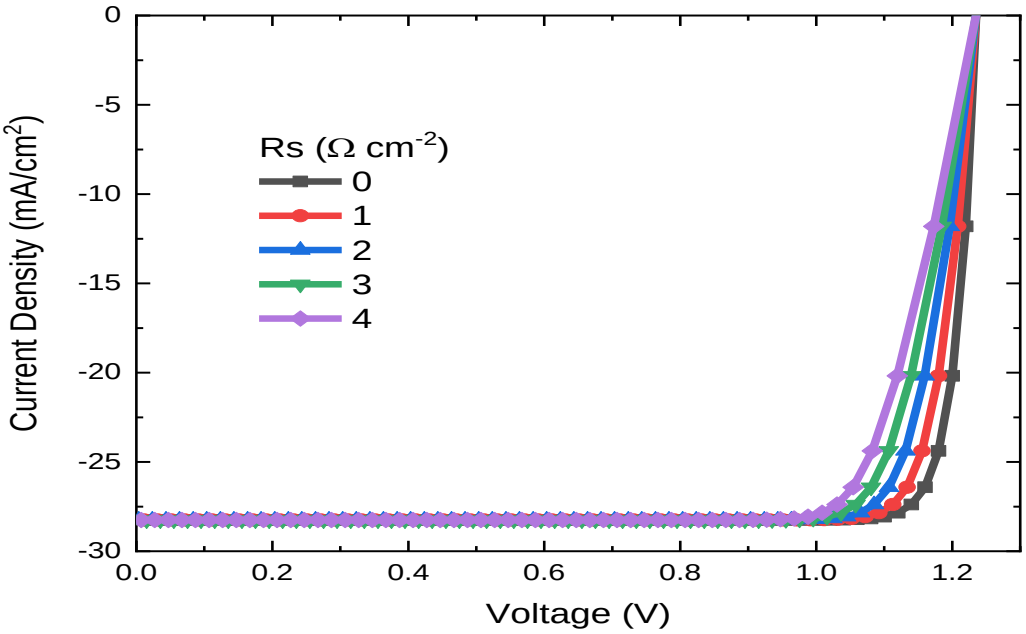

Figure 6 (c) Effect of series resistance on proposed solar cell on current density-voltage.

DOI: https://doi.org/10.70774/ijist.v2i2.23

INTERNATIONAL JOURNAL OF IMMINENT SCIENCE & TECHNOLOGY
Journal homepage: www.ijisnt.com
ISSN:3006-3116
IJIST 2023 Vol-2 Issue-1

3.5. Effect of shunt resistance

The power losses caused by the higher shunt resistance (Rsh) are typically due to manufacturing defects. Low shunt resistance causes power losses in solar cells by providing an alternate current path for the light-generated current. [46,47]. Figure 7 shows the effect of shunt resistance where series resistance was fixed at 0.5Ωm. Shunt resistance was varied from $1x10^2$ to $1x10^8$ Ωm. It is noticeable that in Figure 7(a), all the parameters increased as the shunt resistance increased. Efficiency rises from 18.62% to 30.85%. Similarly, FF, Voc, and Jsc increased from 54.33% to 88.33%, 1.21 to 1.23V, 28.11 to 28.25 mA/cm2. However, it is observed that the parameters became constant from $1x10^6$ to $1x10^8$Ωm.

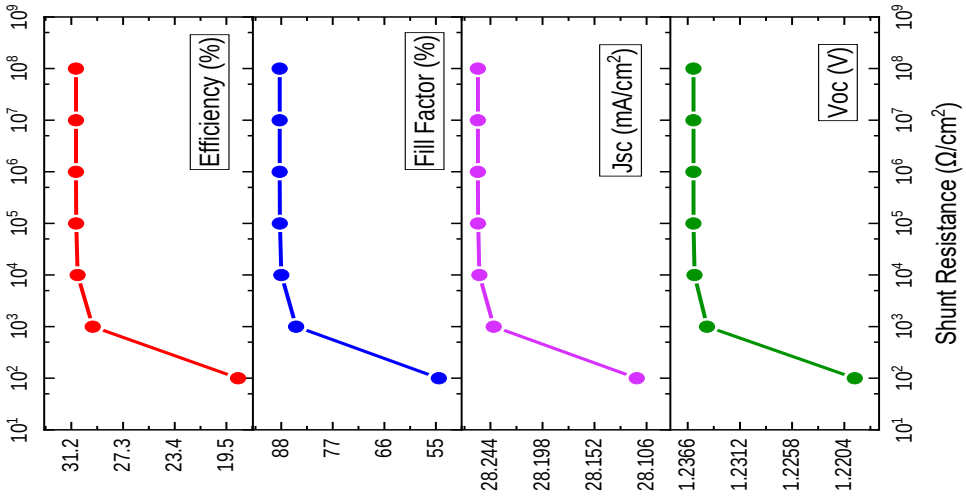

Figure 7(a): Effect of shunt resistance on solar performance parameter

Figure 7(b) shows the effect of shunt resistance on quantum efficiency It is also noticed that the quantum efficiency doesn't change remarkably. [47]. As shunt resistance increases, the current density-voltage curve is improved, as shown in Figure 7(c).

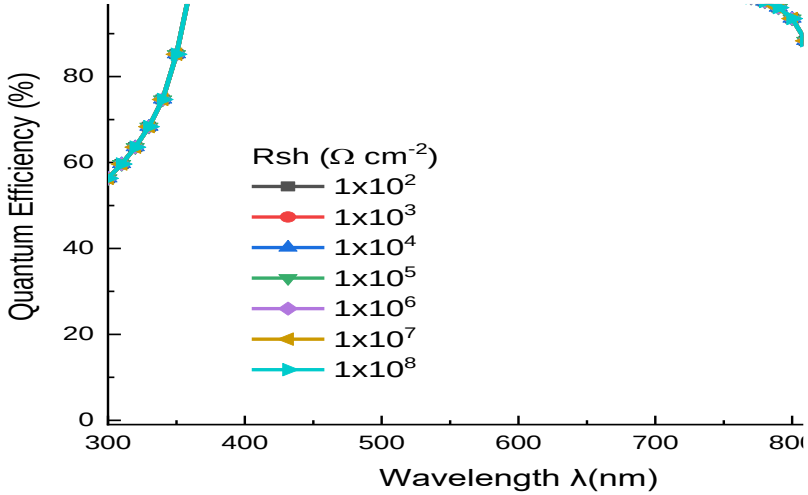

Figure 7(b): Effect of shunt resistance on quantum efficiency.

DOI: https://doi.org/10.70774/ijist.v2i2.23

INTERNATIONAL JOURNAL OF IMMINENT SCIENCE & TECHNOLOGY
Journal homepage: www.ijisnt.com
ISSN.3006-3116

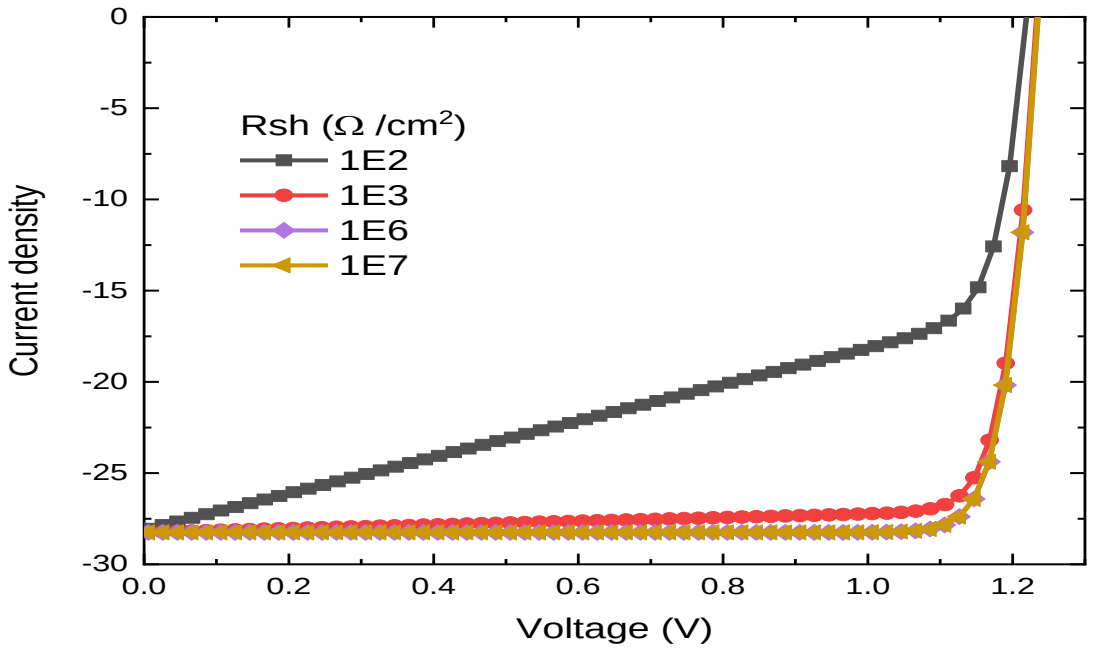

Figure 7(c): Effect of shunt resistance on current density-voltage

3.6. Effect of acceptor doping concentration

The efficiency of a solar cell is significantly affected by the amount of doping used. Doping can be categorized as either n-type or p-type, depending on the dopants used. Thus, improving efficiency relies on setting the appropriate value of N_A [48]. Doping concentration levels can be adjusted experimentally in many different ways [49]. Here, N_A is varied from $1x10^{17}$ to $1x10^{20}$ cm^{-3}. Figure 8 shows the effect of N_A on the proposed solar cell. Table 2 shows the effect of shallow concentration on the proposed cell. Following acceptor doping, holes, and electrons will invariably behave as majority and minority carriers, respectively. Thus, at particular doping of the acceptor atom, the number of hole majority carriers increases, which increases the FF of the device [50]. The increase in V_{OC} of the device is due to the recombination of carriers, which also leads to a gain in power conversion efficiency (η). The equation can also explain the increase in Voc increasing the acceptor density (N_A)

$$V_{OC} = \frac{E_g}{q} - \frac{kT}{q} ln\left[\frac{qD_eN_cN_v}{J_{SC}N_AL_n}\right] \quad (5)$$

Where k denotes the Boltzmann constant, Eg denotes the bandgap energy, T denotes absolute temperature in Kelvin (K), De is the diffusion current of e−, and N_C and N_V represent the density of states of conduction and valence band, respectively. N_A stands for doping acceptor density, Jsc for short circuit current density, and Ln denotes electron diffusion length [51].

For this reason, the JV curve in Figure 8(b) is also improved. There's a negligible change in quantum efficiency, as shown in Figure 8(c).

DOI: https://doi.org/10.70774/ijist.v2i2.23

INTERNATIONAL JOURNAL OF IMMINENT SCIENCE & TECHNOLOGY
Journal homepage: www.ijisnt.com
ISSN.3006-3116
2023 Vol-2 Issue-1

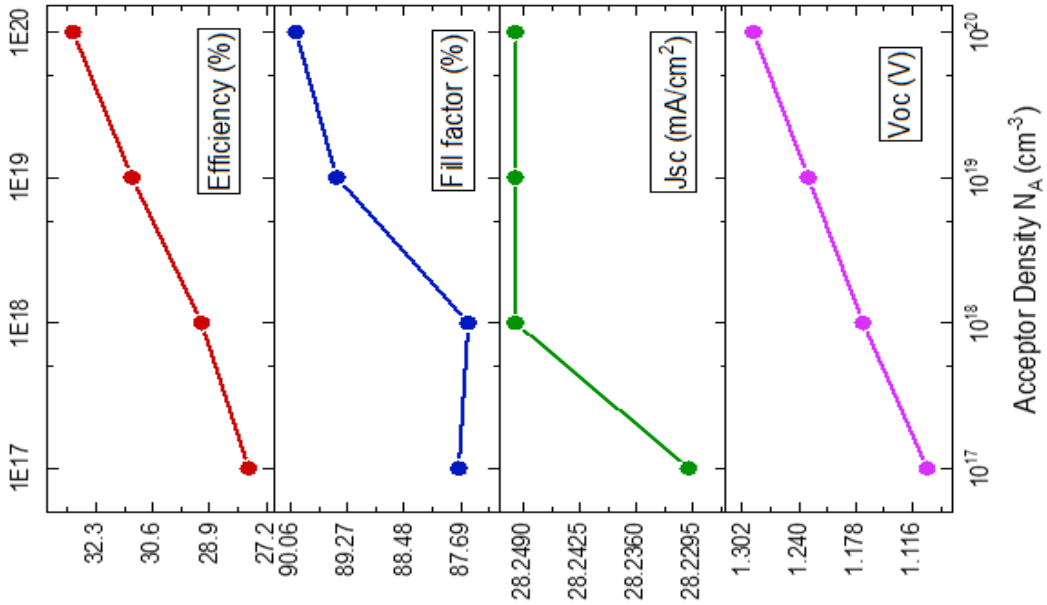

Figure 8(a): Effect of acceptor doping concentration on solar performance parameter

There's a negligible change in quantum efficiency, as shown in Figure 8(b).For this reason, the J-V curve in Figure 8(c) is also improved.

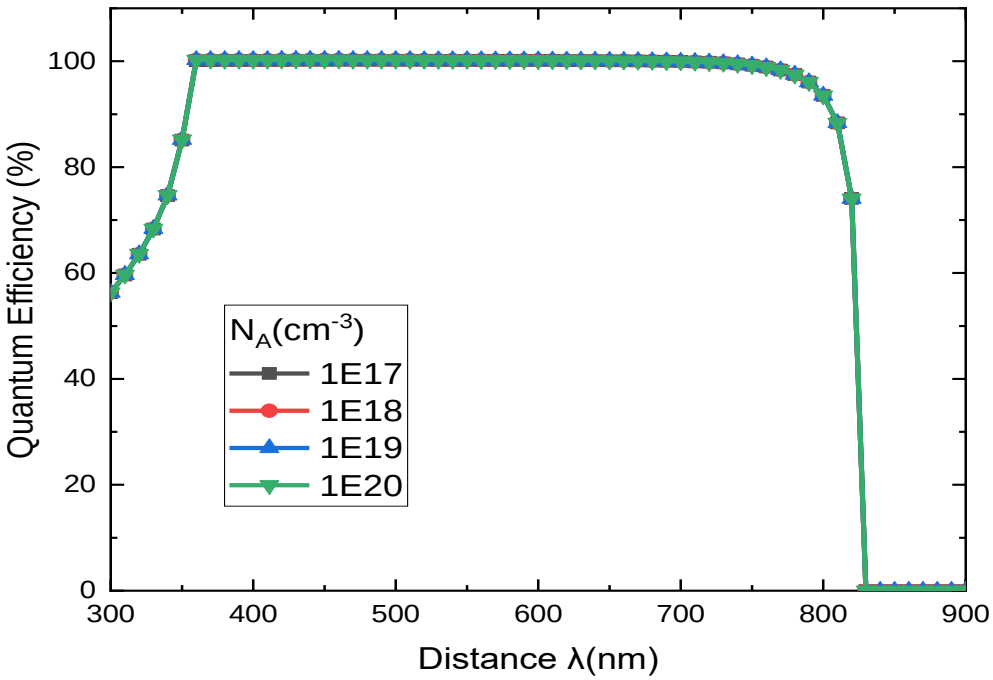

Figure 8(b): Effect of acceptor doping concentration on quantum efficiency.

DOI: https://doi.org/10.70774/ijist.v2i2.23

INTERNATIONAL JOURNAL OF IMMINENT SCIENCE & TECHNOLOGY
Journal homepage: www.ijisnt.com
ISSN.3006-3116
2023 Vol-2 Issue-1

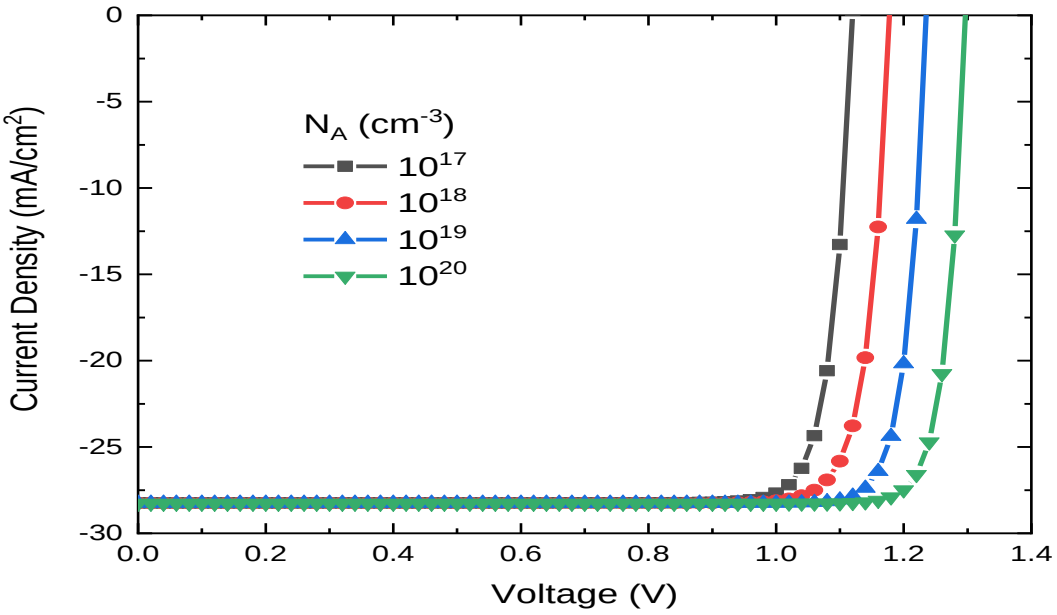

Figure 8(c): Effect of acceptor doping concentration on current density-voltage.

4. Conclusion

In this research, we have proposed an eco-friendly perovskite solar cell structure (ITO/ZnSe/$CsSnGeI_3$/Spiro-MeOTAD/Au). The suggested perovskite solar cell achieves an efficiency of 31.23%. During the simulation, the variation of thickness and defect for the absorber layer is 0.5 to 3µm, 2.45×10^{13} to $2.45\times10^{17}cm^{-3}$. Temperature is varied from 250K to 450K. The variation for series and shunt resistance is 0 to 4 Ω/cm^2 and $1x10^2$ to $1x10^8$ Ω/cm^2. After completing the whole simulation, the optimum thickness for $CsSnGeI_3$ is 1.5µm. For the best performance of solar cells, 300K was obtained. The main aim of the current work is to enhance the thickness of the absorber to obtain the highest efficiency and other output metrics. This perovskite solar cell can be highly recommended for its high efficiency and lead-free. So, the current work of detailed analysis of the Perovskite solar cell device provides a better understanding of the possible fabrication of cost-effective and highly efficient.

4.1 Data Availability

The data supporting the investigation's results are available upon reasonable request from the relevant author.

4.2 Conflicts of Interest

The authors state that they have no conflicts of interest.

4.3 Acknowledgments

The authors would like to express their gratitude to Dr. Marc Burgelman and his colleagues at the Department of Electronics and Information Systems (ELIS), University of Gent, Belgium, for making the SCAPS simulation software available

References

[1]. Rehbein, J. A., Watson, J. E. M., Lane, J. L., Sonter, L. J., Venter, O., Atkinson, S. C., & Allan, J. R. (2020). Renewable energy development threatens many globally important biodiversity areas. Global Change Biology, 26(5), 3040–3051.

[2]. Kannan, N., & Vakeesan, D. (2016). Solar energy for future world: - A review. Renewable and Sustainable

Energy Reviews, 62, 1092–1105.

[3]. Green, M. A., Ho-Baillie, A., & Snaith, H. J. (2014). The emergence of perovskite solar cells. Nature Photonics, 8(7), 506–514.

[4]. Rong, Y., Hu, Y., Mei, A., Tan, H., Saidaminov, M. I., Seok, S. I., ... & Han, H. (2018). Challenges for commercializing perovskite solar cells. Science, 361(6408), eaat8235.

[5[. Tan, Z. K., Moghaddam, R. S., Lai, M. L., Docampo, P., Higler, R., Deschler, F., ... & Friend, R. H. (2014). Bright light-emitting diodes based on organometal halide perovskite. Nature nanotechnology, 9(9), 687-692.

[6]. Ling, Y., Yuan, Z., Tian, Y., Wang, X., Wang, J. C., Xin, Y., ... & Gao, H. (2016). Bright light-emitting diodes based on organometal halide perovskite nanoplatelets. Advanced materials, 28(2), 305-311.

[7]. Kim, Y. H., Cho, H., Heo, J. H., Kim, T. S., Myoung, N., Lee, C. L., ... & Lee, T. W. (2015). Multicolored organic/inorganic hybrid perovskite light-emitting diodes. Advanced materials, 27(7), 1248-1254.

[8]. Dou, L., Yang, Y., You, J., Hong, Z., Chang, W. H., Li, G., & Yang, Y. (2014). Solution-processed hybrid perovskite photodetectors with high detectivity. Nature communications, 5(1), 5404.

[9]. Lee, Y., Kwon, J., Hwang, E., Ra, C. H., Yoo, W. J., Ahn, J. H., ... & Cho, J. H. (2014). High-performance perovskite-graphene hybrid photodetector. Advanced Materials (Deerfield Beach, Fla.), 27(1), 41-46.

[10]. Lyu, M., Yun, J. H., Chen, P., Hao, M., & Wang, L. (2017). Addressing toxicity of lead: progress and applications of low-toxic metal halide perovskites and their derivatives. Advanced Energy Materials, 7(15), 1602512.

[11]. Sun, P. P., Li, Q. S., Feng, S., & Li, Z. S. (2016). Mixed Ge/Pb perovskite light absorbers with an ascendant efficiency explored from theoretical view. Physical Chemistry Chemical Physics, 18(21), 14408-14418.

[12]. Ke, W., & Kanatzidis, M. G. (2019). Prospects for low-toxicity lead-free perovskite solar cells. Nature communications, 10(1), 965.

[13]. Chen, M., Ju, M. G., Garces, H. F., Carl, A. D., Ono, L. K., Hawash, Z., ... & Padture, N. P. (2019). Highly stable and efficient all-inorganic lead-free perovskite solar cells with native-oxide passivation. Nature communications, 10(1), 16.

[14]. Wu, B., Zhou, Y., Xing, G., Xu, Q., Garces, H. F., Solanki, A., ... & Sum, T. C. (2017). Long minority-carrier diffusion length and low surface-recombination velocity in inorganic lead-free CsSnI3 perovskite crystal for solar cells. Advanced Functional Materials, 27(7), 1604818.

[15]. H. Dixit, D. Punetha, S.K. Pandey, Improvement in performance of lead free inverted perovskite solar cell by optimization of solar parameters, Optik 179 (Feb. 2019) 969–976.

[16]. Chung, I., Song, J. H., Im, J., Androulakis, J., Malliakas, C. D., Li, H., ... & Kanatzidis, M. G. (2012). CsSnI3: semiconductor or metal? High electrical conductivity and strong near-infrared photoluminescence from a single material. High hole mobility and phase-transitions. Journal of the american chemical society, 134(20), 8579-8587.

[17]. Chen, M., Ju, M. G., Garces, H. F., Carl, A. D., Ono, L. K., Hawash, Z., ... & Padture, N. P. (2019). Highly stable and efficient all-inorganic lead-free perovskite solar cells with native-oxide passivation. Nature communications, 10(1), 16.

[18]. Xing, G., Mathews, N., Sun, S., Lim, S. S., Lam, Y. M., Grätzel, M., ... & Sum, T. C. (2013). Long-range balanced electron-and hole-transport lengths in organic-inorganic CH3NH3PbI3. Science, 342(6156), 344-347.

[19]. Zhang, A., Chen, Y., & Yan, J. (2016). Optimal design and simulation of high-performance organic-metal halide perovskite solar cells. IEEE journal of quantum electronics, 52(6), 1-6.

[20]. Zhang, F., Wang, Z., Zhu, H., Pellet, N., Luo, J., Yi, C., ... & Grätzel, M. (2017). Over 20% PCE perovskite solar cells with superior stability achieved by novel and low-cost hole-transporting materials. Nano Energy, 41, 469-475.

[21]. Hawash, Z., Ono, L. K., & Qi, Y. (2018). Recent advances in spiro-MeOTAD hole transport material and its applications in organic–inorganic halide perovskite solar cells. Advanced Materials Interfaces, 5(1), 1700623.

[22]. Abdalameer, N. K., Mazhir, S. N., & Aadim, K. A. (2020). The effect of ZnSe Core/shell on the properties of the window layer of the solar cell and its applications in solar energy. Energy Reports, 6, 447-458.

[23]. Dastan, D., Mohammed, M. K., Al-Mousoi, A. K., Kumar, A., Salih, S. Q., JosephNg, P. S., ... & Hossain, M. K. (2023). Insights into the photovoltaic properties of indium sulfide as an electron transport material in perovskite solar cells. Scientific reports, 13(1), 9076.

[24]. Biswas, S. K., Mim, M. K., & Ahmed, M. M. (2023). Design and Simulation of an Environment-Friendly ZrS2/CuInS2 Thin Film Solar Cell Using SCAPS 1D Software. Advances in Materials Science and Engineering, 2023(1), 8845555.

[25]. Kumar, A., & Sharma, P. (2023). Transfer matrix method-based efficiency enhancement of lead-free Cs3Sb2Br9 perovskite solar cell. Solar Energy, 259, 63-71.

[26]. Prasanna, J. L., Goel, E., & Kumar, A. (2023). Numerical investigation of MAPbI3 perovskite solar cells for performance limiting parameters. Optical and Quantum Electronics, 55(7), 610.

[27]. Burgelman, M., Decock, K., Niemegeers, A., Verschraegen, J., & Degrave, S. (2016). SCAPS manual. University of Ghent: Ghent, Belgium.

[28]. Shoewu, O. (2018). Effect of absorber layer thickness and band gap on the performance of CdTe/CdS/ZnO multi-junction thin film solar cell. International Journal o f Advanced Trends in Technology, Management and Applied Science, 4(7), 1-26.

[29]. Ouslimane, T., Et-Taya, L., Elmaimouni, L., & Benami, A. (2021). Impact of absorber layer thickness, defect density, and operating temperature on the performance of MAPbI3 solar cells based on ZnO electron transporting material. Heliyon, 7(3).

[30]. Shoewu, O. (2018). Effect of absorber layer thickness and band gap on the performance of CdTe/CdS/ZnO multi-junction thin film solar cell. International Journal o f Advanced Trends in Technology, Management and Applied Science, 4(7), 1-26.

[31]. Sarker, K., Sumon, M. S., Orthe, M. F., Biswas, S. K., & Ahmed, M. M. (2023). Numerical Simulation of High Efficiency Environment Friendly CuBi2O4-Based Thin-Film Solar Cell Using SCAPS-1D. International Journal of Photoenergy, 2023(1), 7208502.

[32]. Singh, P., & Ravindra, N. M. (2012). Temperature dependence of solar cell performance—an analysis. Solar energy materials and solar cells, 101, 36-45.

[33]. Halim, M. A., Biswas, S. K., Islam, M. S., & Ahmed, M. M. (2022). Numerical Simulation of Non-toxic ZnSe Buffer Layer to Enhance Sb 2 S 3 Solar Cell Efficiency Using SCAPS-1D Software. International Journal of Robotics & Control Systems, 2(4).

[34]. Sunny, A., Rahman, S., Khatun, M., & Ahmed, S. R. A. (2021). Numerical study of high performance HTL-free CH3NH3SnI3-based perovskite solar cell by SCAPS-1D. AIP Advances, 11(6).

[35]. Sherkar, T. S., Momblona, C., Gil-Escrig, L., Avila, J., Sessolo, M., Bolink, H. J., & Koster, L. J. A. (2017). Recombination in perovskite solar cells: significance of grain boundaries, interface traps, and defect ions. ACS energy letters, 2(5), 1214-1222.

[36]. Liu, Y., Stradins, P., Deng, H., Luo, J., & Wei, S. H. (2016). Suppress carrier recombination by introducing defects: The case of Si solar cell. Applied

Physics Letters, 108(2).

[37]. Ball, J. M., & Petrozza, A. (2016). Defects in perovskite-halides and their effects in solar cells. Nature Energy, 1(11), 1-13.

[38]. Biswas, S. K., Sumon, M. S., Sarker, K., Orthe, M. F., & Ahmed, M. M. (2023). A Numerical Approach to Analysis of an Environment-Friendly Sn-Based Perovskite Solar Cell with SnO2 Buffer Layer Using SCAPS-1D. Advances in Materials Science and Engineering, 2023(1), 4154962.

[39]. Ahmad, O., Rashid, A., Ahmed, M. W., Nasir, M. F., & Qasim, I. (2021). Performance evaluation of Au/p-CdTe/Cs2TiI6/n-TiO2/ITO solar cell using SCAPS-1D. Optical Materials, 117, 111105.

[40]. Rono, N., Merad, A. E., Kibet, J. K., Martincigh, B. S., & Nyamori, V. O. (2021). Optimization of Hole Transport Layer Materials for a Lead-Free Perovskite Solar Cell Based on Formamidinium Tin Iodide. Energy Technology, 9(12), 2100859.

[41]. Khan, R., Ahmed, S. F., Khalid, M., & Joshi, B. (2021). Investigating effect of CdS buffer layer on the performance of Cu 2 ZnSnS 4 based solar cells using SCAPS-1D. Transactions on Electrical and Electronic Materials, 22, 177-184.

[42]. Heriche, H., Rouabah, Z., & Bouarissa, N. (2017). New ultra thin CIGS structure solar cells using SCAPS simulation program. International Journal of Hydrogen Energy, 42(15), 9524-9532.

[43]. Al-Mousoi, A. K., Mohammed, M. K., Pandey, R., Madan, J., Dastan, D., Ravi, G., & Sakthivel, P. (2022). Simulation and analysis of lead-free perovskite solar cells incorporating cerium oxide as electron transporting layer. RSC advances, 12(50), 32365-32373.

[44]. Chakraborty, K., Choudhury, M. G., & Paul, S. (2019). Numerical study of Cs2TiX6 (X= Br−, I−, F− and Cl−) based perovskite solar cell using SCAPS-1D device simulation. Solar Energy, 194, 886-892.

[45]. Chami, R., Lekdadri, A., Omari, L. H., Hlil, E. K., & Chafi, M. J. M. T. E. (2021). Investigation of the photovoltaic properties of BaHf1-xZrxS3 (x≤ 1) chalcogenide perovskites using first principles calculations. Materials today energy, 20, 100689.

[46]. Simya, O. K., Mahaboobbatcha, A., & Balachander, K. (2015). A comparative study on the performance of Kesterite based thin film solar cells using SCAPS simulation program. Superlattices and Microstructures, 82, 248-261.

[47]. Khan, R., Ahmed, S. F., Khalid, M., & Joshi, B. (2021). Investigating effect of CdS buffer layer on the performance of Cu 2 ZnSnS 4 based solar cells using SCAPS-1D. Transactions on Electrical and Electronic Materials, 22, 177-184.

[48]. Dastan, D., Mohammed, M. K., Al-Mousoi, A. K., Kumar, A., Salih, S. Q., JosephNg, P. S., ... & Hossain, M. K. (2023). Insights into the photovoltaic properties of indium sulfide as an electron transport material in perovskite solar cells. Scientific reports, 13(1), 9076.

[49]. Bag, A., Radhakrishnan, R., Nekovei, R., & Jeyakumar, R. (2020). Effect of absorber layer, hole transport layer thicknesses, and its doping density on the performance of perovskite solar cells by device simulation. Solar Energy, 196, 177-182.

[50]. Srivastava, P., Rai, S., Lohia, P., Dwivedi, D. K., Qasem, H., Umar, A., ... & Baskoutas, S. (2022). Theoretical study of perovskite solar cell for enhancement of device performance using SCAPS-1D. Physica Scripta, 97(12), 125004.

[51]. Heriche, H., Rouabah, Z., & Bouarissa, N. (2017). New ultra thin CIGS structure solar cells using SCAPS simulation program. International Journal of Hydrogen Energy, 42(15), 9524-9532.